Journal of Solid State Chemistry **153,** 342–348 (2000)
doi:10.1006/jssc.2000.8780, available online at http://www.idealibrary.com on IDEAL®

A Novel Sonochemical Method for the Preparation of Nanophasic Sulfides: Synthesis of HgS and PbS Nanoparticles

Junjie Zhu,*,† Suwen Liu,* O. Palchik,* Yuri Koltypin,* and A. Gedanken*,[1]

*Department of Chemistry, Bar-Ilan University, Ramat-Gan 52900, Israel; and †Department of Chemistry, Nanjing University, Nanjing, 210093, China

Received February 18, 2000; accepted May 18, 2000; published online July 26, 2000

HgS and PbS nanoparticles of about 15 and 20 nm in size have been prepared by the sonochemical irradiation of an ethylenediamine solution of elemental S and mercury acetate or lead acetate under air. The nanoparticles are characterized using techniques such as transmission electron microscopy, X-ray diffraction, absorption spectroscopy, diffuse reflection spectroscopy, and energy-dispersive X-ray analysis. © 2000 Academic Press

Key Words: **HgS; PbS; sonochemistry; nanoparticles.**

1. INTRODUCTION

Nanocrystalline semiconductors have electronic properties intermediate between those of molecular entities and macrocrystalline solids and are at present the subject of intense research (1–5). Nanometric semiconductor particles exhibit novel properties due to the large number of surface atoms and/or the three-dimensional confinement of electrons. Altering the size of the particle alters the degree of confinement of the electrons and the electronic structure of the solid state. In particular, there are "band edges" which are tunable with particle size. Nanoparticles of semiconductors have many potential applications in the area of demonstration devices, such as light-emitting diodes (6, 7), photocatalysts (8), and electrochemical cells (9).

Nanocrystallites have been prepared by several different synthetic methods (1–5, 9) many involving aqueous solution. However, for the majority of technologically important semiconductors, such methods have some limitations in practice, especially in the use of noxious compounds such as H_2S.

Currently, the sonochemical method has been used extensively to generate novel materials with unusual properties (10), since they form particles of a much smaller size and higher surface area than those reported by other methods. The chemical effects of ultrasound arise from acoustic cavitation, that is, the formation, growth, and implosive collapse of bubbles in a liquid. The implosive collapse of the bubbles generates a localized hotspot through adiabatic compression or shock wave formation within the gas phase of the collapsing bubble. The conditions formed in these hotspots have been experimentally determined, with transient temperatures of ~ 5000 K, pressures of 1800 atm (11), and cooling rates in excess of 10^{10} K/s. These extreme conditions attained during bubble collapse have been exploited to decompose the metal–carbonyl bonds and generate metals (11–14), metal carbides (15), and metal oxides and sulfides (16–19).

There has been much interest in the synthesis and physical characterization of the II–VI family of nanoscale semiconductors. Most studies in this field were focused on cadmium sulfide and zinc sulfide (20–22). However, owing to the toxicity problem of mercury, only a few references reported mercury sulfide synthesis (23, 24). Mercury sulfide crystallizes in three different structures. Of these three phases, trigonal (α-HgS) and sphalrite-type HgS (β-HgS) have been explored the most. Thin layers of mercury sulfide have been prepared by evaporation and sputtering methods (24–26). HgS is a useful material in fields such as ultrasonic transducers, image sensors, electrostatic image materials, and photoelectric conversion devices (23, 25). PbS is also one of the most attractive mineral sulfides for a wide variety of applications, e.g., IR detectors and Pb^{2+} ion-selective sensors. Various processes, such as sintering precipitation, vacuum evaporation, and electrochemical deposition, have been employed to produce PbS bulk material or PbS film (27–29). Qingxi Lu *et al.* reported the preparation of PbS nanoparticles in an autoclave with average sizes of 90 and 55 nm (30). It is also worth mentioning that nanophased sulfides have been prepared previously using ultrasonic waves. For example, Suslick and co-workers have sonicated a slurry of molybdenum hexacarbonyl and sulfur in an isodurene solution and have obtained MoS_2 (31). The sonochemical formation of Q-state CdS colloids and the dissolution of larger colloidal CdS particles have also been described (32).

In this paper, we report the use of a sonochemical method for the preparation of nanophased HgS and PbS. They are

[1]To whom correspondence should be addressed. E-mail: gedanken@mail.biu.ac.il. Fax: + 972-3-5351250.

0022-4596/00 $35.00

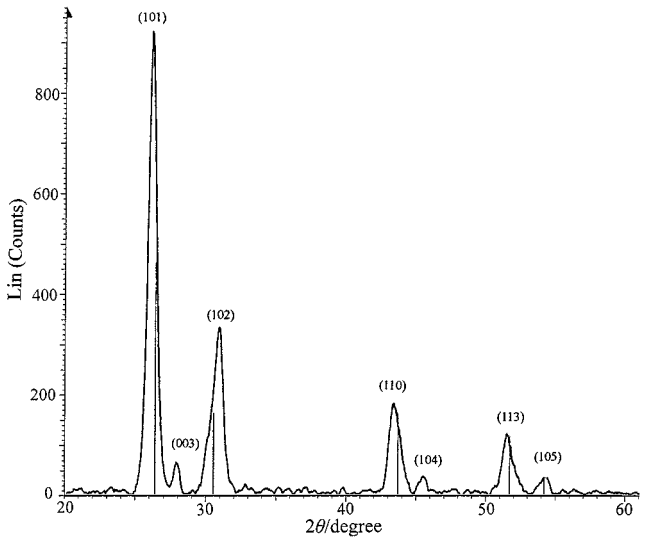

FIG. 1. XRD patterns of HgS nanoparticles.

synthesized by sonicating an ethylenediamine solution of 1-decanethiol (RSH, $R = CH_3(CH_2)_9$) and the corresponding acetates. The sonication resulted in HgS and PbS nanoparticles which are approximately 15 and 20 nm in size, respectively, as calculated using the Debye–Scherer formula. Similar sizes are also obtained from the TEM images. The nanoparticles are also characterized using powder X-ray diffraction (XRD), UV–visible spectroscopy, diffuse reflection spectroscopy (DRS), transmission electron microscopy (TEM), and X-ray photoelectron spectroscopy (XPS).

2. EXPERIMENTAL

A. Materials

$Hg(Ac)_2$ (99.9%), $Pb(Ac)_2.2H_2O$, elemental S, and 1-decanethiol (96%) were purchased from Aldrich and used without further purification. Doubly distilled water was used. The absolute ethanol which was used was purchased from Pharmco Products. Ultrasonic irradiation was accomplished with a high-intensity ultrasonic probe (Misonix, XL Sonifier, 1.13 cm diameter Ti horn, 20 Hz, 60 W cm^{-2}).

B. Instruments

The instruments used in this report for TEM and EDAX measurements have been described elsewhere (17–19). The instruments employed for other measurements will be described herein.

(1) Absorption spectra are recorded on a Hewlett Packard 8453 UV–visible spectrophotometer.
(2) The powder X-ray diffraction patterns are recorded using a Bruker D8 advance diffractometer.
(3) Diffuse reflection spectroscopy (DRS) measurements are carried out on a Cary (Varian IE) spectrophotometer.

C. Preparation of HgS and PbS Nanoparticles

In the presence of RSH (200 mg), 230 mg of $Hg(Ac)_2$ and 23 mg of elemental S are dissolved in 70 ml of ethylenediamine and are sonicated for 1 h in the open air, at

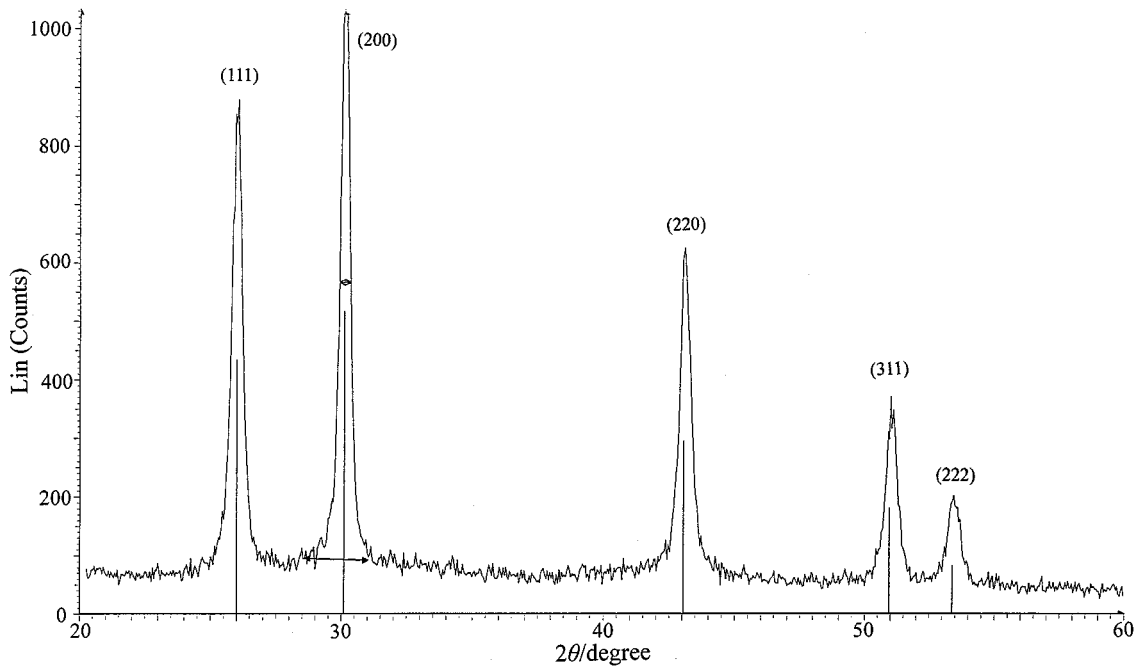

FIG. 2. XRD patterns of PbS nanoparticles.

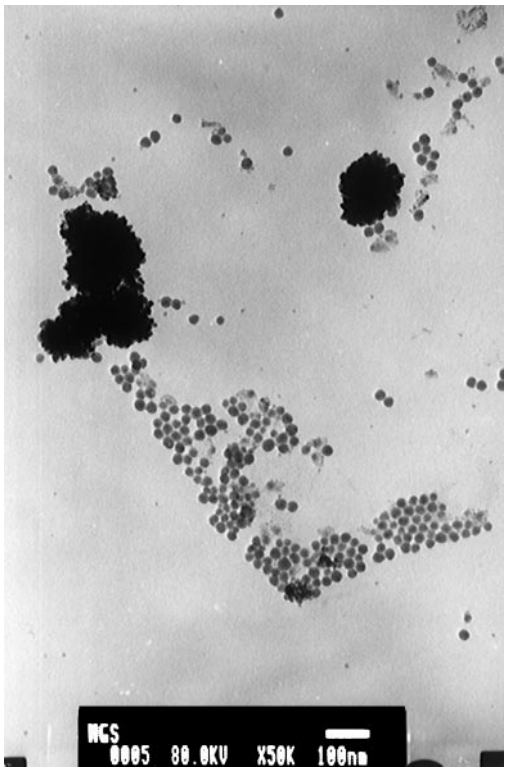

FIG. 3. TEM images of HgS nanoparticles.

room temperature. A round-bottom Pyrex glass vessel (total volume 70 ml) is used for the ultrasound irradiation. After sonication for 1 h, the solution is centrifuged and the precipitate washed with water and then with absolute ethanol. Black powder is obtained. A similar method is performed in the preparation of PbS nanoparticles (260 mg of $Pb(Ac)_2.2H_2O$ and 22 mg of elemental S are dissolved in 70 ml of ethylenediamine in the presence of RSH).

D. XRD, EDX, and TEM Studies

The XRD pattern of the as-prepared HgS shows the presence of broad peaks (Fig. 1). Diffraction peaks corresponding to the (101), (003), (102), (110), (104), (113), and (105) planes of sphalrite-type HgS (β-HgS) are detected. The broad peaks indicate that the crystal size is small. The size of HgS nanoparticles estimated from the Debye–Scherrer formula is 15 nm. The XRD pattern of the as-prepared PbS also exhibits broad peaks (Fig. 2). The diffraction peaks correspond to the (111), (200), (220), (311), and (222) planes of sphalrite-type PbS. The size of the PbS nanoparticles estimated from the Debye–Scherrer formula is 20 nm.

The EDAX pattern for HgS shows the presence of Hg and S peaks with an average atomic ratio Hg : S of 56 : 44. This results points out that the samples are rich in Hg. In the case of PbS, the EDAX curve reveals the presence of Pb and S, with an average atomic ratio Pb : S of 43 : 57.

The morphology of HgS nanoparticles is studied by transmission electron microscopy (TEM). Figure 3 shows the image of the HgS nanoparticles. In the picture, we find that a large part of the as-prepared particles are monodispersed. It is apparent that HgS nanoparticles are spherical. The average size of these nanoparticles is in the range of 10–15 nm, which is in good agreement with the XRD result. In the picture we also find another part of the HgS particles which is aggregated. The TEM measurements of the as-prepared PbS nanoparticles are shown in Fig. 4. The morphology of the nanoparticles is close to a rectangular shape and the average dimensions are ca. 20×15 nm.

E. Optical Properties

The UV–visible absorption spectra (Fig. 5) of HgS nanoparticles dispersed in ethanol solution show a broad absorption peak centered at about ca. 500 nm. The band can be attributed to a surface state of HgS nanoparticles because the absorption lies below the absorption edge of the particles. The large fraction of surface atoms present in these nanoparticles leads to the large number of dangling bonds and stoichiometric or external defects originating from the surface transition (33–35).

We have also measured the optical diffuse reflection spectrum of HgS powder in order to resolve the excitonic or

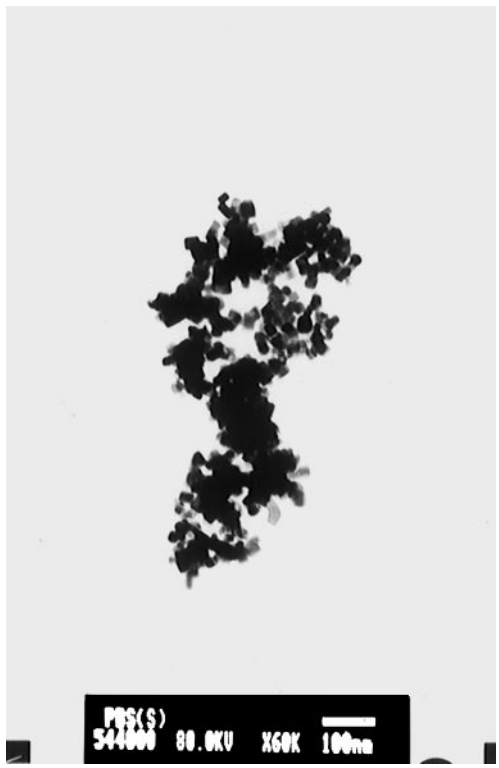

FIG. 4. TEM images of PbS nanoparticles.

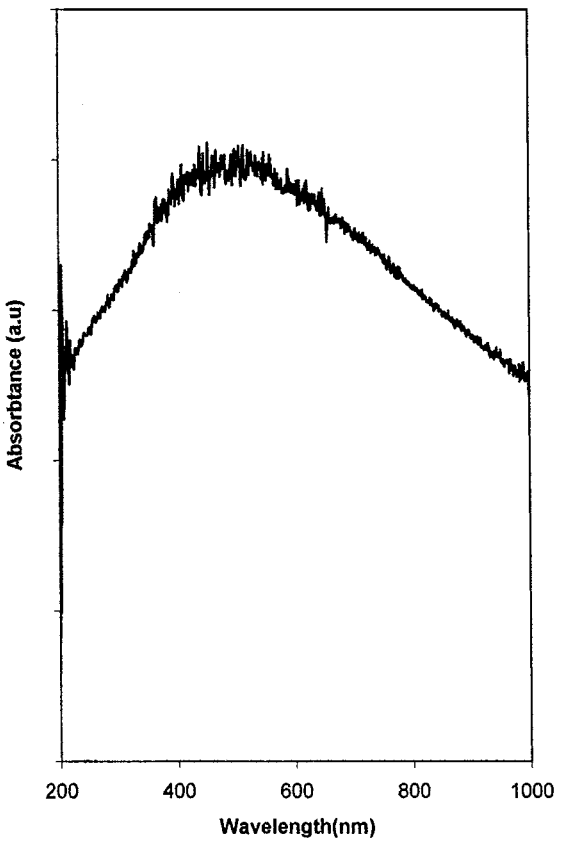

FIG. 5. Absorption spectrum of an ethanol solution of HgS nanoparticles.

interband (valence conduction band) transitions of HgS, which allows us to calculate the bandgap. Figure 6a depicts the optical diffuse reflection spectrum of the HgS powder. An estimate of the optical bandgap is obtained using the following equation for a semiconductor,

$$\alpha(v) = A(h'v/2 - Eg)^{m/2},$$

where $h' = h/2\pi$, α is the absorption coefficient, and m is equal to 1 for a direct allowed transition. Since α is proportional to $F(R)$, the Kubelka–Munk function, the energy intercept of a plot of $(F(R)hv)^2$ versus hv, yields Eg for a direct allowed transition (Fig. 6b) (36). From the spectra the bandgap of HgS is calculated as ca. 2.40 eV. The value of the bandgap energy is slightly larger than that of the reported value for bulk HgS (ca. 2.0 eV) (23). The increase in the magnitude of the bandgap may be indicative of size quantization (18).

F. XPS Studies

Figure 7 shows the high-resolution XPS spectra of S(2*p*) and Pb(4*f*) taken for the Pb and S regions of the as-prepared samples. The peaks at 161.8 eV and 160.8 eV correspond to the S(2*p*) transitions, and the peaks at 142.6 eV and 137.7 eV correspond to the Pb(4*f*) binding energy. Similar results were obtained in Ref. (37). The peak areas of the Pb and S cores are measured and yield a ratio of Pb to S of 43 : 57, which is in good agreement with EDAX results.

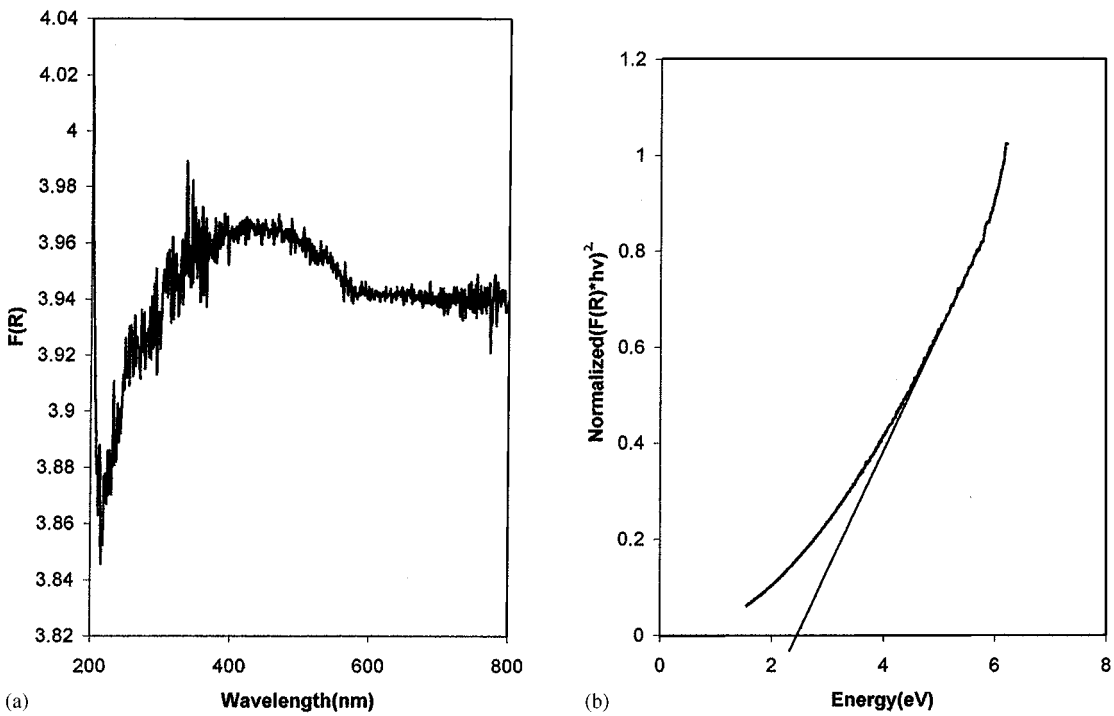

FIG. 6. (a) Diffuse reflection spectrum of a glass coated with HgS nanoparticles. (b) Normalized $(F(R)hv)^2$ versus hv (eV) of HgS nanoparticles.

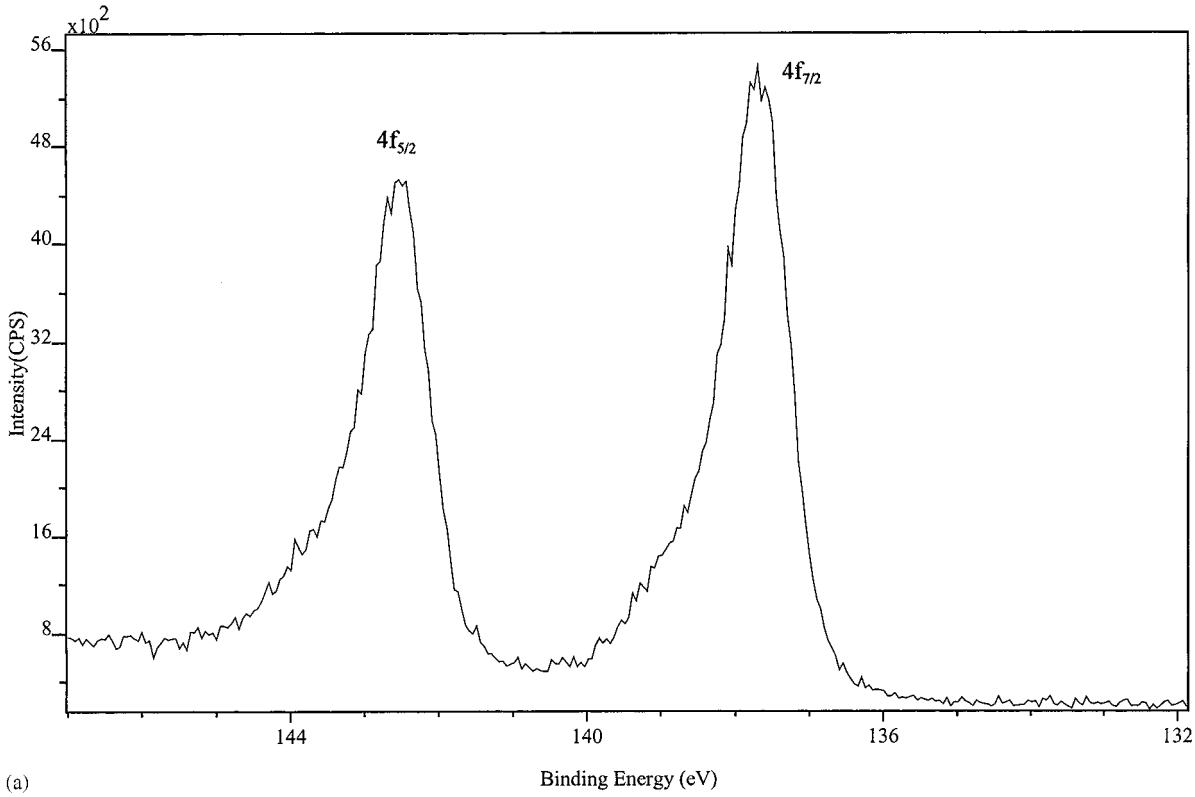

(a)

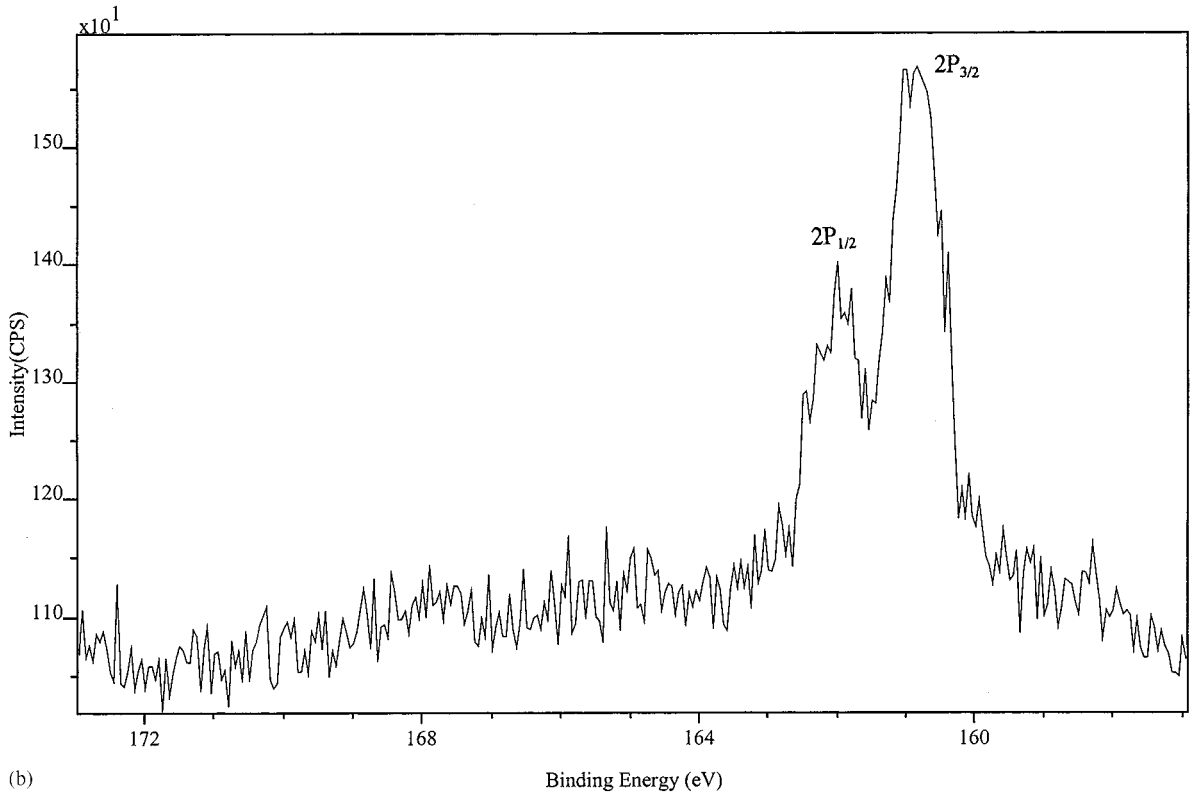

(b)

FIG. 7. High-resolution XPS spectra taken for the Pb and S regions of PbS.

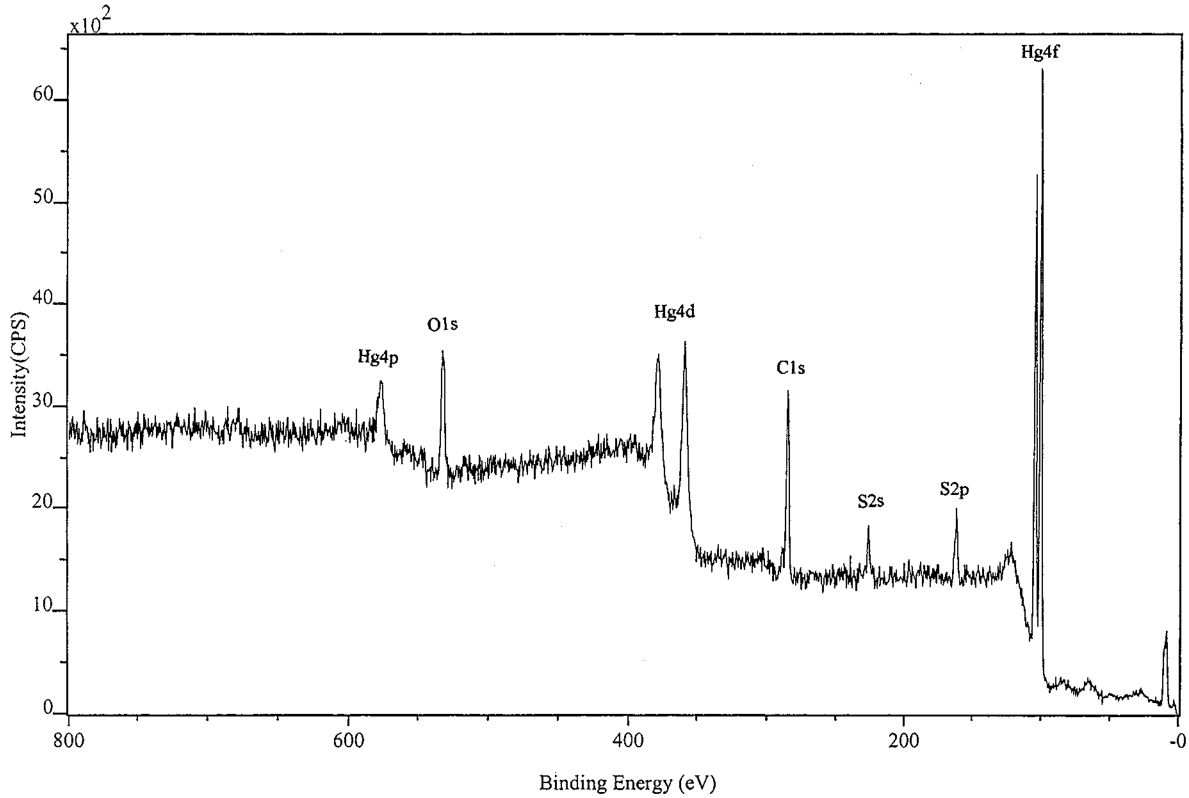

FIG. 8. Wide XPS pictures of the as-prepared HgS.

For HgS, the XPS spectrum provides further evidence for the formation of HgS as the sole product. Figure 8 shows wide XPS spectra of HgS. The two strong peaks in the high-resolution XPS spectra taken for the Hg region at 101 eV and 104.90 eV are assigned to the Hg(4*f*) binding energy (41). The peaks in the high-resolution XPS spectra measured in the S energy region are detected at 162.0 eV and 163.5 eV and are attributed to the S(2*p*) (37, 41) transitions. Peak areas of the Hg and S cores are measured and have a ratio of Hg to S of 55 : 45, which is also in good agreement with the EDAX results.

Ultrasonic waves which are intense enough to produce cavitation can drive chemical reactions such as oxidation, reduction, dissolution, and decomposition (10). Other reactions, such as the promotion of polymerization, have also been reported to be induced by ultrasound.

In the current experiments, we have found that the use of RSH is essential in the preparation of PbS and HgS nanoparticles. In the case of PbS, if the reaction is conducted in the absence of RSH, although PbS is formed, the particles size are larger than those in the presence of RSH. Figure 9 shows the PbS TEM image obtained in the absence of RSH. It shows that the size of the as-prepared particles is large, about 100–200 nm. A control reaction in which only RSH (without elemental S) and $Pb(Ac)_2$ are sonicated has not led to the formation of PbS. The result of this sonication was a yellow precipitate. Its nature has not yet been characterized, but according to Ref. (38), the yellow precipitate may indicate the presence of a complex compound with a thiol ligand, $\{Pb(SR)\}_n^{n+}$. We propose the formation of PbS as the result of the following steps. The first is a reaction leading to the formation of a complex, rather than a solid phase. The second, sulfur in ethylenediamine, can produce H_2S. Ultrasonic waves can promote this reaction. The reaction may be as follows (41):

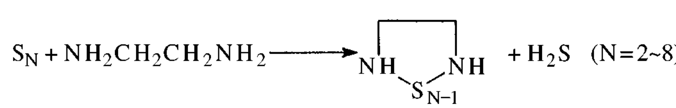

The third, the complex formed in the first stage, reacts with H_2S to produce PbS nanoparticles. Lelieur *et al.* (39) and Parkin *et al.* (40) have reported the formation of the active sulfur species in the formation of metal sulfides in liquid ammonia. Y.D. Li *et al.* (41) reported the formation of HgS nanoparticles by reacting HgO and sulfur for 6–16 h, while it takes only 1 h to obtain HgS by using ultrasonic waves. In the sonochemical reaction system, the ethylenediamine may play an important role in generating the active sulfur species. Another result of our experiments was the finding that different concentrations of 1-decanethiol could affect the particle's size. In the case of PbS, the higher concentrations of the thiol led to smaller particles. This result is in accord with the literature report (42).

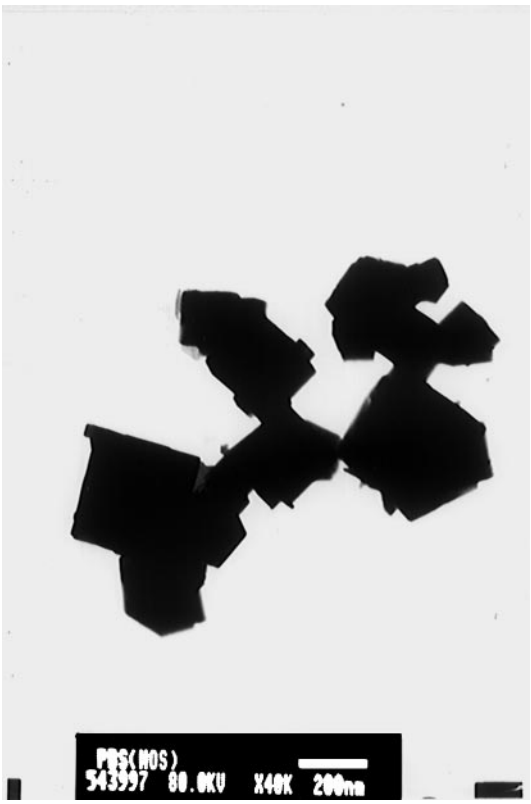

FIG. 9. TEM images of PbS nanoparticles in the absence of RSH.

3. CONCLUSION

HgS and PbS nanoparticles have been prepared by the sonochemical method in the presence of 1-decanethiol. In this work we found that 1-decanethiol and ethylenediamine are very important in the synthesis of these semiconductor nanoparticles. The advantage of this process is that it is a simple and efficient method to produce nanoparticles that are small in size. We can foresee the upscaling of the process to form large quantities of these kinds of nanomaterials.

ACKNOWLEDGMENTS

Prof. A. Gedanken thanks the German Ministry of Science through the Deutche-Israeli Program (DIP) for its support and gratefully acknowledges receipt of a NEDO International Joint Research Grant. Dr. Zhu and Dr. Liu thank the Kort 100 Scholarship Foundation for supporting their postdoctoral fellowships. Drs. Zhu and Liu are also grateful for the support of the China Scholarship Council. The authors are grateful to Mr. G. Salitra for his help in the XPS measurements. The kind assistance of Dr. Siguang Chen and Dr. A. Zaban is gratefully acknowledged. We also thank Dr. Shifra Hochberg for editorial assistance.

REFERENCES

1. D. Dounghong, J. Ramsden, and M. Gratzel, *J. Am. Chem. Soc.* **104,** 29777 (1982).
2. R. Rossetti, J. L. Ellison, J. M. Gibson, and L. E. Brus, *J. Chem. Phys.* **80,** 4464 (1984).
3. A. Henglein, *Chem. Rev.* **89,** 1861 (1989).
4. Y. Wang and N. Herron, *J. Phys. Chem.* **95,** 525 (1991).
5. H. Weller, *Adv. Mater* **5**, 88 (1993).
6. B. O. Dabbousi, M.G. Bawendi, O. Onitsuka, and M. F. Rubner, *Appl. Phys. Lett.* **66**, 1361 (1995).
7. V. L. Colvin, M. C. Schlamp, and A. P. Alivisators, *Nature* **370,** 354 (1994).
8. C. K. Gratzel and M. Gratzel, *J. Am. Chem. Soc.* **101,** 7741 (1979).
9. A. Hangfeldt and M. Gratzel, *Chem. Rev.* **95,** 49 (1995).
10. K. S. Suslick, "Ultrasound: Its Chemical, Physical and Biological Effects." VCH, Weinheim, 1988.
11. K. S. Suslick, S. B. Choe, A. A. Cichowlas, and M. W. Grinstaff, *Nature* **353,** 414 (1991).
12. Yu. Koltypin, G. Katabi, R. Prozorov, and A. Gedanken, *J. Non-Cryst. Solids* **201,** 159 (1996).
13. Y. Nagata, Y. Mizukoshi, K. Okitsu, and Y. Maeda, *Radiat. Res.* **146,** 333 (1996).
14. K. Okitsu, Y. Mizukoshi, H. Bandow, Y. Maeda, T. Yamamoto, and Y. Nagata, *Ultrason. Sonochem.* **3,** 249 (1996).
15. T. Hyeon, M. Fang, and K. S. Suslick, *J. Am. Chem. Soc.* **118,** 5492 (1996).
16. X. Cao, Yu. Koltypin, G. Katabi, I. Felner, and A. Gedanken, *J. Mater. Res.* **12,** 405 (1997).
17. N. Arul Dhas and A. Gedanken, *J. Phys. Chem. B* **101,** 9495 (1997).
18. J. J. Zhu, S. T. Aruna, Yu. Koltypin, and A. Gedanken, *Chem. Mater.* **12,** 143 (2000).
19. J. J. Zhu, Yu. Koltypin, and A. Gedanken, *Chem. Mater.* **12,** 73 (2000).
20. C. B. Murray, D. J. Norris, and M. G. Bawendi, *J. Am. Chem. Soc.* **155,** 8706 (1993).
21. M. Forment, H. Cachet, H. Essaaidi, G. Maurin, and R. Cortes, *Pure Appl. Chem.* **69,** 77 (1997).
22. K. Sooklal, B. S. Cullum, S. M. Angel, and C. J. Maurphy, *J. Phys. Chem.* **100,** 4551 (1996).
23. S. S. Kale and C. D. Lokhande, *Mater. Chem. Phys.* **59,** 242 (1999).
24. M. Z. Najsoski, I. S. Grozdanov, S. K. Dey, and B. B. Siracevska, *J. Mater. Chem.* **8,** 10 (1998).
25. N. Tokyo, *J. Appl. Phys.* **46,** 4857 (1975).
26. N. Tokyo, *J. Appl. Phys.* **48,** 3405 (1977).
27. M. Sharon, K. S. Ramaiah, M. Kumar, M. Neumann-Spallart, and C. Levy-Clement, *J. Electroanal. Chem.* **436,** 49 (1997).
28. F. C. Meldrum, J. Flath, and W. Knoll, *J. Mater. Chem.* **9,** 711 (1999).
29. R. Thielsch, T. Bohme, R. Reiche, D. Schlafer, H.-D. Bauer, and H. Botteher, *Nanostruct. Mater.* **10,** 131 (1998).
30. Q. Y. Lu, J. Q. Hu, K. B. Tang, Y. T. Qian, X. M. Liu, and G. Zhou, *J. Solid State Chem.* **146,** 484 (1999).
31. M. M. Mdleleni, T. Hyeon, and K. S. Suslick, *J. Am. Chem. Soc.* **120,** 6189 (1998).
32. J. Z. Sostaric, R. A. Caruso Hobson, P. Mulvaney, and F. Grieser, *J. Chem. Soc., Faraday Trans.* **93,** 1791 (1997).
33. W. Chen, Z. Wang, Z. Lin, and L. Lin, *J. Appl. Phys.* **82,** 3111 (1997).
34. D. Hayes, O. I. Micic, M. T. Nenadovic, V. Swayambunathan, and D. Meisel, *J. Phys. Chem.* **93,** 4603 (1989).
35. V. Swayambunathan, D. Hayes, K. Schmit, K. H. Schmidt, Y. K. Liao, and D. Meisel, *J. Am. Chem. Soc.* **112,** 3831 (1990).
36. V. Luca, S. Djajanti, and R. F. Howe, *J. Phys. Chem. B* **102,** 10650 (1998).
37. M. Takahashi, Y. Ohshima, K. Nagata, and S. Furuta, *J. Electroanal. Chem.* **359,** 281 (1993).
38. V. S. Gurin, *J. Crystal Growth* **191,** 161 (1998).
39. P. Dubois, J. P. Lelieur, and G. Lepoutre, *Inorg. Chem.* **28,** 195 (1989).
40. G. Henshaw, I. P. Parkin, and G. A. Shaw, *J. Chem. Soc., Dalton Trans.* 231 (1997).
41. Y. D. Li, Y. Ding, H. L. Giao, and Y. T. Qian, *J. Phys. Chem. Solids* **60,** 958 (1999).
42. C.-H. Fischer and A. Henglein, *J. Phys. Chem.* **93,** 5578 (1989).